Research Article

Jan Dupuis*, Christoph Holst, Heiner Kuhlmann

Laser Scanning Based Growth Analysis of Plants as a New Challenge for Deformation Monitoring

DOI 10.1515/jag-2015-0028
received November 23, 2015; accepted December 09, 2015.

Abstract: Nowadays, the areal deformation analysis has become an important task in engineering geodesy. Thereby, not only manmade objects are of high interest, also natural objects, like plant organs, are focused more frequently. Thus, the analysis of leaf growth, i. e. the spatial development of the leaf surface, can be seen as a problem of deformation monitoring. In contrast to classical geodetic tasks, the absolute size of the deformation of the leaf surface is small, but usually great compared to the object size. Due to the optical characteristics of leaf surfaces, the point clouds, commonly acquired with high precision close-up laser scanners, provide a point-to-point distance that is small or equal compared to the measurement accuracy. Thus, the point clouds are usually processed and the leaf area is derived from a triangulation-based surface representation (mesh), resulting in a significant uncertainty of area calculation. In this paper, we illustrate the lacks of the mesh-based leaf area calculation. Using high precision gauge blocks as well as a number of tomato leaves, uncertainties of the area derivation are revealed and evaluated. The application of a B-spline approximation illustrates the advantages of an approximation-based approach and introduces the prospect for further research.

Keywords: Close-up Laser Scanning, Plant Growth Analysis, Plant Phenotyping, Non-parametric Deformation Analysis

1 Introduction

In this section, the relevance of plant phenotyping as well as the connection between plant phenotyping and deformation analysis is addressed, followed by the aim of the study.

1.1 Relevance of Plant Phenotyping

Due to the increase of the world's population and the resulting food scarcity, the breeding of high quality plants has become an important tool to counteract the world hunger problems [22]. Plant breeding is focused on developing new types of plants – so called genotypes – that are more resistant against several environmental impacts like draught stress, nutrient availability as well as biotic and abiotic stress [8]. The response of the plant to environmental conditions is not only a functional reaction [9]. Thus, a change in growth rate of fast developing crops or vegetables is a sensitive and direct indicator of stress [17]. In this context, plant phenotyping describes the acquisition of functional and spatial characteristics of genotypes under specific environmental conditions.

1.2 Relation to Deformation Analysis

Plant phenotyping, especially the monitoring of plant growth, can be addressed as a deformation analysis. Thereby, the plant can be seen as a *multiple input multiple output – system* (MIMO), where the input values describe the environmental conditions and the output values are growth parameters like the leaf area or other phenotypic parameters. The spatial change of a plant combines both types of deformation, i. e., rigid body movements and changes in shapes and dimension [2]: rigid body movements due to a movement of the whole leaf and changes in shape and dimension due to the growth. We only consider the latter type of deformation here. This deformation can be analyzed in one of the common deformation models [11]. A classical phenotypic growth analysis is evaluated in an identity- or a static deformation model, depending on whether additional information, e. g. about water or nutrient supply, are available [19] or not [21]. The spatial

***Corresponding author: Jan Dupuis,** Institute of Geodesy and Geoinformation, University Bonn, Nussallee 17, 53115 Bonn, Germany, e-mail: dupuis@igg.uni-bonn.de
Christoph Holst, Heiner Kuhlmann, Institute of Geodesy and Geoinformation, University Bonn, Nussallee 17, 53115 Bonn, Germany, e-mail: c.holst@igg.uni-bonn.de, heiner.kuhlmann@uni-bonn.de

development of a plant is usually described by growth parameters like leaf area or convex hull volume, derived from 3D point clouds measured with different 3D imaging systems [19, 21].

1.3 Aim of the Study

One of the most frequently applied growth parameters is the leaf area. Usually, the leaf area is derived from a triangulation-based surface interpolation, a so-called mesh, using processed point clouds of various 3D imaging systems [1, 14, 19]. In this study, we want to illustrate the lacks of the deformation analysis using the leaf area as growth parameter, derived from a meshed surface. Using high precision gauge blocks as well as leaves of a five of tomato plants, we show the dependency of the leaf area on the processing of the point cloud. The application of an approximation-based approach using uniform B-splines improves the area derivation for the gauge block measurements and also for the leaf area calculation.

Hence, the need of using an approximation-based approach with a freeform parameterization instead of using the mesh-based approach for modeling leafs is highlighted in this study. These considerations can be transferred to other kinds of deformations analyses of natural objects.

2 Data Acquisition

In the first two subsections the technical measuring setup and the special characteristics of leaf measurements are addressed, followed by a description of the data processing and the derivation of the leaf area.

Because phenotyping on organ level is mostly performed using young plants (leaf area < 2500 mm²) and the growth rate is often small (only a few mm² per day), measurements were performed with a high precision industrial measuring system.

2.1 3D Laser Scanner for Leaf Surface Acquisition

The laser scanning device used in this study is a combination of the triangulation-based 2D close-up laser scanner "ScanWorks V5" from Perceptron company and a 7 DoF articulated measuring arm "Infinite 2.0" from ROMER company. This measuring system provides a 3D point repeatability of 45 μm and a 3D length accuracy of 69 μm, defined as maximum permissible error (mpe). The laser scanner works according to the light section method [4] and is able to measure 7640 points per profile with a maximum profile frequency of 60 Hz in a field of view of ~105 mm × 110 mm (middle measuring range). This results in point resolution of ~14 μm within one laser line. Due to the combination of the laser scanner and the measuring arm, the small measuring range of the scanner is extended to a spherical measuring volume with a diameter of ~2.8 m.

2.2 Measuring Leaves Surfaces with Lasers

Measuring plant development using commercial high precision laser devices is not trivial at all. Compared against most of the manmade objects plants provide some special characteristics that have to be taken into account:

1. The complexity of the plant structure,
2. the movement of the plant and
3. penetration of the laser beam.

The complexity of the plant mainly affects the completeness of the resulting point cloud. Despite using a sensor with highest flexibility, it is not always possible to achieve an occlusion free point cloud of the whole plant surface. Depending on the species and the age of the plant, the leaf structure is more or less complex resulting in an overlapping of leaves or an occlusion of the stem structure.

The movement of the plant can be separated into movements caused by the flow of the air and the proper motion of plants, the so called plant tropism [9]. While the plant tropism causes a rigid body movement between two measuring epochs, the movement of the air provokes a swinging of the leaf mainly manifesting in high measuring noise. Thus, the parameters estimated for the growth analysis should be rotation- and translation- invariant and should be able to handle a poor signal-to-noise ratio.

The accuracy of the point cloud is also affected by the special optical properties of the leaf surface. Leaf surfaces consist of different layers providing different optical properties [20]. Thus, the emitted laser line is able to penetrate the leaf surface and to interact with the photoactive leaf tissue content, the chlorophyll, resulting in a partial absorption of the emitted laser ray [6]. While the absorption leads to a weakening of the received measuring signal and therefore, to higher measuring noise [5] or a signal that is not evaluable, the penetration into the leaf structure causes a systematic deviation of the distance measurement. This systematic deviation is not constant. It rather depends on the type of the plant as well as on the physiological state [6].

Beside the reduced accuracy, the point cloud shows an irregular point distribution, cause by the hand-operated measuring system. Within one scanline the point-to-point distance is nearly constant with a magnitude of about 14 μm. In contrast, the distance between two consecutive scanlines strongly depends on the moving speed of the operator. Thus, to achieve a complete point cloud of the leaf surface it has to be scanned several times with different orientations of the laser line. Furthermore, the distance between two adjacent points is usually small compared to the measuring noise.

All these aspects affect the resulting point cloud and have to be considered in the processing step before data analysis.

2.3 Processing of the Point Cloud

The processing of the point clouds usually consists of three main steps [18, 19, 20]. These processing steps were performed using the commercial software Geomagic Studio and Geomagic Control (3D Systems, USA).

In the first step, outliers like scanning artefacts, caused by overexposure of the sensor, and objects that do not belong to the plant were removed manually from the raw point cloud.

In a second step, the point cloud of the plant was separated manually into points representing single leaves and stem points. Theoretically, this step can be replaced by an automatic classification procedure, like Surface Feature Histograms [18]. However, we decided to use a manual labeling process because the automatic algorithm already requires a processed point cloud with a regular point distribution.

To provide a regular point distribution, in the third step, the point clouds were thinned out using the algorithm provided by Geomagic Control software. Thereby, the software reduces the number of points as long as the defined minimum point-to-point distance is reached. Against algorithms like noise reduction or surface smoothing, thinning only eliminates a subset of points as long as the defined point distribution is reached. Thus, the remaining point cloud contains a reduced number of raw data points.

2.4 Derivation of the Leaf Area

From the separated and regularly distributed point cloud, a mesh was calculated. Thereby, the data points were interpolated by a network of triangles following the fundamentals of the Delaunay triangulation [3].

The interpolation was performed using the algorithm implemented in Geomagic Control without any smoothing options, so that every vertex in the mesh represents a raw data point of the point cloud. Using this representation, it is possible to calculate the leaf area by summing up the area of all faces of the mesh.

3 Theoretical Impact of Point Cloud Processing on the Area Derivation

Because a mesh depicts an interpolation of neighboring surface points, the presence of measuring noise has to be taken into account. Figure 1 **A** shows a cross section of a surface and the measured point cloud. The distance between two neighboring points is partially small compared to measuring noise as it can be expected for measurements performed with the appointed scanning device. Meshing the raw point cloud data results in connection of all neighboring points (red line) and, therefore, in an area that is derived to large. Thinning the point cloud, i. e. reducing the number of points (green and blue line), causes a kind of surface smoothing and results in a smaller area derivation that is closer to the real area. However, an extensive smoothing also reduces the level of detail.

Another effect that has to be regarded, concerns the boundary of the surface (Figure 1 **B**). Because the algorithm tries to keep most boundary points, the larger the point-to-point distance is set in the thin-out procedure, the smoother the boundary is interpolated and the larger the area is derived. However, this effect is expected to be small compared to the aforementioned one.

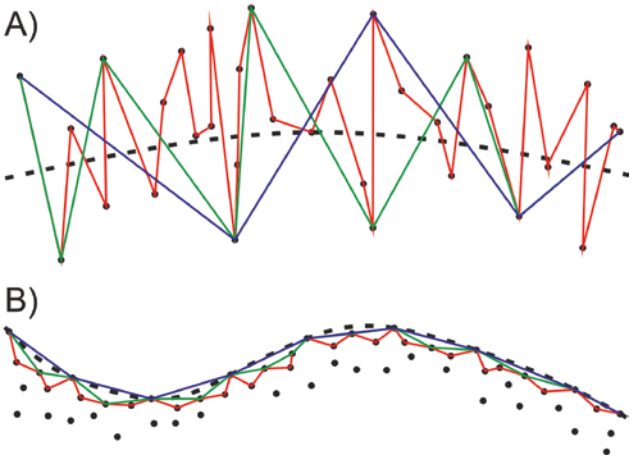

Figure 1: A) Cross section of a surface and the measured point cloud. **B)** Topview of the boundary of a surface. The colored lines represent the interpolation for an increasing thinning level (R < G < B).

4 Laboratory Investigations with Gauge Blocks

As aready written, in most studies the leaf area is calculated based on a mesh-based approach whose weak accuracy is revealed by the present study. This is proven, in the first step, by laboratory investigations based on gauge blocks. In the second step, the results are transferred to the derivation of leaf areas (see Section 5). Both times, the results of the mesh-based approach are compared to the ones of an approximation-based approach using B-Splines.

4.1 Experimental Setup

To provide a reference for the area, we used a set of gauge blocks with a deviation from the nominal value of $0.10 + 0.0002 \cdot L\ \mu m$ (tolerance), where L equals the nominal length of the gauge block in millimeter. The width of the blocks was measured using a micrometer screw with an accuracy of 0.01 mm (1σ).

Five blocks of different size were setup as shown in Figure 2 and measured consecutively under controlled environmental conditions. To analyze the repeatability of the approach, every gauge block was measured 27 times. The resulting point clouds were processed as described in Section 2.2 and different thinning levels ranging from 0.1 mm up to 0.8 mm point-to-point distance were generated. After the generation of the mesh, the surface area was calculated for every repetition (see Section 2.4).

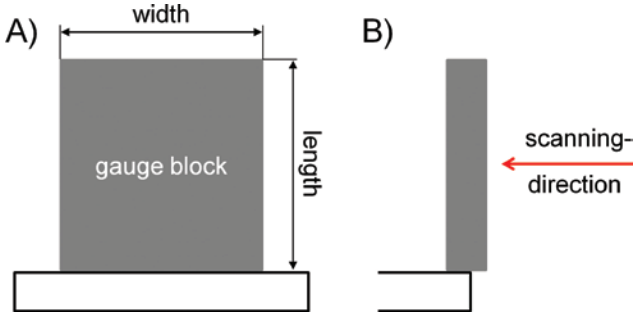

Figure 2: A) Front and **B)** side view of the measuring setup.

4.2 Results of the Mesh-based Area Derivation

In Table 1, representative results of a gauge block with a dimension of 30 x 34.95 mm², i. e. a nominal area of 1048.5 mm², are shown. It can be seen that the calculated area varied with the defined thinning level. The calculation performed on the raw point cloud resulted in an area that was about 5 % larger compared to reference value. The larger the point-to-point distance was chosen, the smaller the area was calculated. Furthermore, the standard deviation of the 27 repetitions was higher in case of no thinning and 0.1 mm thinning and reached about 3 mm² for larger point distances. The minimum deviation from the reference area was obtained at a thinning of 0.4 mm. However, these results are not generally applicable. As we used gauge blocks of different sizes ranging from 331.5 mm² to 2446.5 mm², larger areas showed partially different behavior. While the trend – the stronger the thinning process the smaller the calculated area – pertained for all tested objects, the minimum deviation from the nominal value was reached for different thinning levels. For smaller blocks, the minimum deviation was obtained for a thinning with a point-to-point distance of 0.4 mm and for larger blocks at 0.8 mm and more.

The results support the theoretical considerations in Section 3. The thinning of the point cloud causes a smoothing and, therefore, the derived area decreases with an increasing point-to-point distance. The averaged area values for 0.5 mm to 0.8 mm thinning are even smaller than the reference area. This effect can be attributed to the thinning procedure. Large thinning leads to reduction of important edge points and points at the corners of the gauge block resulting too small area values.

Table 1: Averaged area of a 30 x 34.95 mm² gauge block for different thinning levels ranging from no thinning to a point-to-point distance of 0.8 mm.

	reference area: 1048.5 mm² (± 0.3 mm²)								
	raw data	0.1 mm	0.2 mm	0.3 mm	0.4 mm	0.5 mm	0.6 mm	0.7 mm	0.8 mm
avg. area [mm²]	1100,013	1073,480	1056,827	1051,389	1048,511	1046,523	1045,108	1043,338	1042,920
std.–dev. [mm²]	9,780	5,654	3,490	3,039	3,002	2,593	2,900	2,942	2,627
std.–dev. [%]	0,9 %	0,5 %	0,3 %	0,3 %	0,3 %	0,2 %	0,3 %	0,3 %	0,3 %
ref.–act. [mm²]	−51,513	−24,980	−8,327	−2,889	−0,011	1,977	3,392	5,162	5,580
ref.–act. [%]	−4,9 %	−2,4 %	−0,8 %	−0,3 %	0,0 %	0,2 %	0,3 %	0,5 %	0,5 %

4.3 Approximation-based Area Derivation

In order to avoid the interpolation of a noisy point cloud as it is done in the mesh-based approach, the surface is approximated this time. Then, the adjusted scan points are used to calculate the area. The representation of freeform surfaces can be realized by approximation approaches like NURBS. Due to the flat surface of the gauge blocks, we applied an approximation using B-spline as a simplification of NURBS. This procedure is explained in the following in more detail.

4.3.1 B-spline Approximation

B-splines have shown their applicability in geodetic applications, e. g. for the analysis of ground movements in height networks [12], and also in non-geodetic applications like the analysis of fractured surfaces in material research [23] or for the approximation of leaf surfaces [10, 15].

The representation of a curve by splines is based on the piecewise approximation with polynoms of grade *n*. The extension of the one dimensional curve in a second direction enables the approximation of the surface points *P(x,y)* using the tensor product

$$P(x,y) = \sum_{i=0}^{N-1} \sum_{j=0}^{M-1} P_{i,j} \cdot N_i^n(x) \cdot M_j^m(y), \quad (1)$$

Where $P_{i,j}$ are the knot points, N and M depict the basis function of grade n and m in x- and y-direction, respectively. A further detailed description of splines can be found in Niemeier [16], Heunecke et al. [11] as well as Harmening and Neuner [10].

For the generation of the knot points for the piecewise approximation, the point clouds of the gauge blocks were rotated into their principle axes and a regularly distributed xy-grid was calculated. In this preliminary approach the number of knot points was chosen in a way, that the coarse leaf structure is modeled adequate. After the estimation of the spline parameters using a Gauss-Markov model, adjusted observations were derived with a point-to-point distance of 0.1 mm. The area was limited by the boundary points of the point cloud extracted by an alpha shape approach [7]. Using the best-fitting point clouds, meshes were calculated and the area was derived as described in Section 2.3.

To compare the results to the existing approach, all point clouds of the different thinning levels, generated with Geomagic Control were approximated by spline surfaces.

4.3.2 Results of the Approximation-based Area Derivation

Due to the approximation, the adjusted point clouds as well as the generated meshes provided a much smoother surface compared to the raw or thinned point clouds. This also manifested in the results of the area calculation. For all investigated gauge blocks, the standard deviation of the random samples was nearly constant for all thinning levels providing only a small dispersion. Regarding the magnitude, the smaller blocks (~340 mm²) resulted in a standard deviation of 0.9 % while the larger blocks (~1000 up to ~2500 mm²) provided a standard deviation of 0.4 %. This is only slightly higher than the mesh-based interpolation but independent from the point distribution and density of the point cloud.

Another difference concerns the deviation of the calculated area values from the nominal ones. For the mesh-based approach, the minimum deviation from the nominal area value was reached for different thinning levels depending on the size of the gauge block (see Section 4.2). Using splines, with the exception of the largest block, the smallest deviations from the nominal value were obtained for the approximation of the raw point cloud data, with a magnitude of less than 1 % for all tested block sizes. Similar to the mesh-based results the derived area decreased with an increasing point-to-point distance. However, the impact of the thinning procedure is much smaller.

These results imply that the approximation-based approach is more robust against the point distribution and density as well as against the presence of measuring noise.

4.4 Comparison of the Mesh- and the Approximation-based Approach

Calculating the surface area from a mesh-based surface representation requires a processing of the point cloud, in order to avoid an overestimation of the area. Due to presence of measuring noise, unprocessed point clouds result in a highly structured mesh and, therefore, in an area that is too large compared to nominal area. To counteract this effect the point clouds have to be thinned out. However, this thinning procedure has to be adapted to the overall size of the object, because larger areas need a larger point-to-point distance to provide a minimum deviation from the nominal area (see Section 4.2).

Using an approximation-based approach, the minimum deviation from the nominal area was achieved for raw point cloud data. Thus, the derived area is independent of the thin-out procedure with a deviation of less than 1%.

Furthermore, the standard deviation of the random samples is constant for different point densities and distributions. As shown in Section 4.2.3, the area calculation based on the approximation-based approach is more reliable and accurate for the investigated point-to-point distances.

5 Derivation of the Leaf Area

In this section, the results of the mesh-based and the approximation-based approaches used for the derivation of leaf areas of tomato plants are illustrated.

5.1 Results of the Mesh-based Leaf Area Derivation

To check, whether the effects revealed for the gauge blocks are directly transferable to plant measurements, a random sample of five tomato plants measured over a period of 7 days was analyzed using the mesh-based approach.

Contrary to the laboratory investigation with gauge blocks, in case of leaf surfaces no nominal area values were available. Thus, we were only able to analyze the variation of the leaf surface for different thinning levels.

Principally, the calculated leaf area for the different thinning levels followed a similar trend as it was found for the gauge blocks. The larger the point-to-point distance at the thin-out procedure was chosen, the smaller the leaf area was derived. However, there were significant differences that have to be stated here.

First of all, calculating the leaf area using the raw point cloud data sometimes resulted in area values that were smaller compared to the areas calculated from the thinned point clouds. Because of the reduced measuring accuracy and the systematic deviations (see Section 2.2) the ratio of measuring noise and point-to-point distance became worse resulting in too highly creased edges which in turn leads to perforated surface mesh (Figure 3).

Another difference concerns the decrease of the leaf area with an increasing point-to-point distance: While the reduction of the gauge blocks was relatively small, e. g. around 5% for the data presented in Table 1, the mean decrease of the leaf area was about 30%, averaged over all five tomato plants and all measuring dates. Furthermore, the trend of the reduction was not constant. It differed for every single leaf of a plant and changed with every new measuring epoch.

This uncertainty in the leaf area calculation, of course, affected the derivation of the growth. The absolute growth of the leaf area was calculated from the difference of two area values of two consecutive measuring epochs using the same thinning level. Thereby, the growth for the different thinning levels varied significantly (Figure 4). Due to the inconsistent decrease of the leaf area with increasing thinning level, the growth was also not constant for a single leaf. In most of the cases, the variation of the absolute growth was great compared to the mean growth value (cf. leaves no. 2 and 4 in Figure 4), averaged from all thinning levels. In some cases, the range of the variation even exceeded the mean growth value. Consequently, small deformations, as they were expected for daily measurements, were not statistically detectable.

These results clearly reveal that the mesh-based approach used in many studies does not lead to reliable and accurate estimates of the leaf growth.

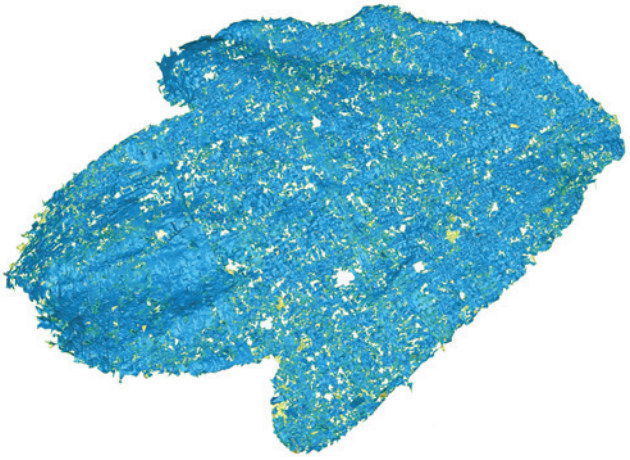

Figure 3: A mesh calculated from raw point cloud data providing a perforated surface representation.

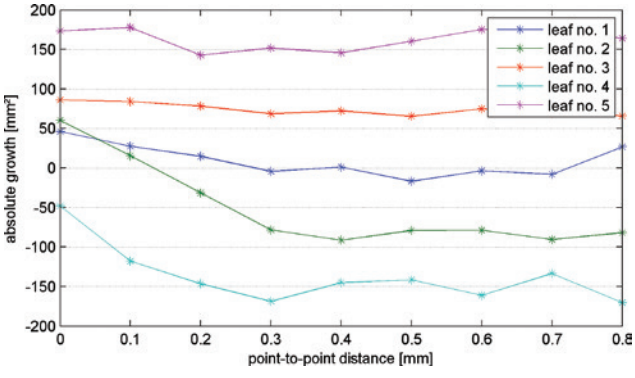

Figure 4: Absolute growth, i. e. the difference between the areas of two consecutive days, of one representative plant at different thinning levels.

5.2 Application of B-splines to Leaf Surfaces

Applying the B-spline approach, appointed in Section 4.3.1, to leaf surfaces imposes some requirements on the shape of the leaf surface. Because the approximation is performed on a planar grid, the leaf surface should not provide high curvature. Furthermore, boundary points should be clearly extractable by the used alpha shape approach, i. e. deep leaf indentations may cause a systematic deviation. To illustrate the general applicability of splines for the derivation of leaf areas, we approximated one leaf, providing a surface with small curvature and only small leaf indentations. The approximation was performed on different thinning levels in order to compare the results to the mesh-based approach.

In Figure 5, the deviations between the approximated leaf surface and the raw point cloud are illustrated. The distribution of the deviations shows that the approximation represents the rude shape of the leaf. However, smaller details, like leaf veins, were smoothed. Finally, the comparison resulted in a standard deviation of 91 μm.

As described in Section 4.3.1, the area was calculated from meshes generated from the adjusted point clouds of the spline approximation. The results of both approaches (Table 2) show that the derived leaf area differs significantly. Comparable to the results in Section 5.1, the leaf area of the mesh-based approach decreased considerably (about 25 %) for the different thinning levels. In contrast, the leaf area of the approximation-based approach varied only little. The decrease reached only about 4 % between the smallest and the largest point-to-point distance. Furthermore, due to the smoothing of the spline approximation, the magnitude of the area was smaller for all thinning levels.

Table 2: Comparison of the mesh-based and the B-spline-based leaf area.

thinning level	mesh-based [mm²]	approx.-based [mm²]
raw data	710,727	551,269
0.1 mm	729,872	549,898
0.2 mm	648,709	547,888
0.3 mm	613,970	545,136
0.4 mm	592,005	542,049
0.5 mm	581,631	537,482
0.6 mm	574,069	537,974
0.7 mm	567,416	532,309
0.8 mm	578,672	531,608
range	151,200	19,661
range / avg.	24,3 %	3,6 %

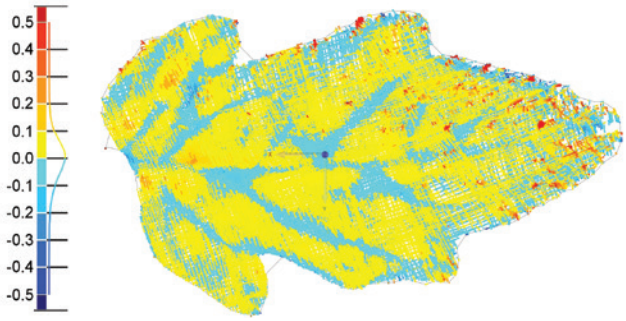

Figure 5: Deviations [mm] between the B-spline approximation and the raw point cloud data.

Despite the promising results for the appointed leaf, there are limitations regarding the shape of the approximated leaf. As described in the beginning of this section, the uniform implementation of the B-splines, defined on a planar grid with equidistant knot points, restricts the maximum curvature of the leaf. For the approximation of arbitrary leaves, the grid has to be adapted to the shape of the leaf surface as it is described for example in Harmening and Neuner [10] by using Coons patch.

6 Conclusion

The investigations illustrated the lacks of the mesh-based approach, commonly used for the calculation of the leaf area from 3D point clouds. Laboratory experiments with high precision gauge blocks revealed deviations from the nominal area values varying with the thinning level, i. e. the defined point-to-point distance, as well as with the absolute size of the measured surface. This effect got reinforced on plant surfaces due to the reduced measuring accuracy. Leaf area variations caused by different thinning levels reached a magnitude of 30 % of the mean leaf area on average (see Section 5.1). For the purpose of a deformation analysis, this uncertainty, as a result of data processing, exacerbates the reliable detection of leaf growth.

An improvement for the area calculation was obtained for the approximation with uniform B-splines. For the gauge blocks, the minimum deviation from the nominal values was reached by approximating the raw point cloud data and the variations caused by different point-to-point distances became small.

Promising results were also obtained for the B-spline approximation of leaf surfaces. However, the uniform implementation of the splines prevented the general applicability on arbitrary leaf surfaces. However, non-uniform implementations of B-splines like NURBS may

improve the approximation of arbitrary, highly curved 3D leaf surface shapes and, thus, can improve the leaf area calculation and, therefore, the deformation analysis.

The investigations have shown the significance for the development of a freeform surface representation of natural objects like leaves surfaces. The difficulty of such a development is characterized in Holst and Kuhlmann [13]. First promising results for the approximation of leave surfaces were obtained by Harmening and Neuner [10].

Acknowledgements: The authors also want to express their gratitude to Florian Zimmermann and Johann Christian Rose for their assistance in data acquisition.

References

[1] Bellasio, C., Olejníčková, J., Tesař, R., Šebela, D., and Nedbal, L. (2012). Computer reconstruction of plant growth and chlorophyll fluorescence emission in three spatial dimensions. *Sensors*, 12(1), 1052–1071.De Lange, N. (2013). Geoinformatik: in Theorie und Praxis. 3. Auflage, Springer-Verlag, Berlin Heidelberg.

[2] Chrzanowski, A., Frodge, S. L., Avella, S. (1993). The worldwide status of monitoring and analysis of dam deformations. In: Proceedings of 7th International Symposium on Deformation Measurements together with 6th Canadian Symposium on Mining Surveying, Banff, Alberta, pp. 77–88.

[3] Delaunay, B. (1934). Sur la sphere vide. *Bulletin der Akademischen Wissenschaften der UdSSR, Klasse der Mathematik und Naturwissenschaften*, pp. 793–800.

[4] Donges, A., and Noll, R. (1993). Lasermeßtechnik. Grundlagen und Anwendungen. Hüthig Verlag, Heidelberg, pp. 214–237.

[5] Dupuis, J., and Kuhlmann, H. (2014). High-Precision Surface Inspection: Uncertainty Evaluation within an Accuracy Range of 15 µm with Triangulation-based Laser Line Scanners. *Journal of Applied Geodesy*, 8(2), pp. 109–118.

[6] Dupuis, J., Paulus, S., Mahlein, A.-K., Kuhlmann, H., Eichert, T. (2015). The Impact of different Leaf Surface Tissues on active 3D Laser Triangulation Measurements. *Photogrammetrie-Fernerkundung- Geoinformation, 2015(6)*, pp. 437–448.

[7] Edelsbrunner, H., and Mücke, E. P. (1994). Three-dimensional alpha shapes. *ACM Transactions on Graphics (TOG) 13.1*, pp. 43–72.

[8] Furbank, R. T., and Tester, M. (2011). Phenomics–technologies to relieve the phenotyping bottleneck. *Trends in plant science,* 16 (12), pp. 635–644.

[9] Gilroy, S. (2008). Plant tropisms. *Current Biology*, 18(7), pp. R275–R277.

[10] Harmening, C. and Neuner, H. (2015). A constraint-based parameterization technique for B-spline surfaces. *Journal of Applied Geodesy, 9(3)*, pp. 143–161.

[11] Heunecke, O., Kuhlmann, H., Welsch, W., Eichhorn, A. and Neuner, H. (2013). Handbuch Ingenieurgeodäsie. Auswertung geodätischer Überwachungsmessungen. 2. Auflage, Wichmann Verlag Heidelberg.

[12] Holst, C. and Kuhlmann, H. (2015). Mathematische Modelle zur flächenhaften Approximation punktweise gemessener Bodensenkungen auf Basis von Präzisionsnivellements. In: *Busch, W., Niemeier, W., Neumann, I. (Hrsg.): Geomonitoring 2015*, Clausthal-Zellerfeld, pp. 189–206.

[13] Holst, C. and Kuhlmann, H. (2016). Challenges and present fields of action at laser scanner based deformation analysis. 3rd Joint International Symposium on Deformation Monitoring (JISDM), Wien, Austria.

[14] Hosoi, F., Nakabayashi, K., and Omasa, K. (2011). 3-D Modeling of tomato canopies using a high-resolution portable scanning lidar for extracting structural information. *Sensors* 11 (2), pp. 2166–2174.

[15] Kempthorne, D. M., et al. (2015). Surface reconstruction of wheat leaf morphology from three-dimensional scanned data. *Functional Plant Biology 42.5*, pp. 444–451.

[16] Niemeier, W. (2008). Ausgleichungsrechnung: Statistische Auswertemethoden. 2. Auflage, Walter de Gruyter, Berlin, New York.

[17] Omasa, K., Hosoi, F., and Konishi, A. (2007). 3D lidar imaging for detecting and understanding plant responses and canopy structure. *Journal of experimental botany,* 58 (4), pp. 881–898.

[18] Paulus, S., Dupuis, J., Mahlein, A. K., and Kuhlmann, H. (2013). Surface feature based classification of plant organs from 3D laserscanned point clouds for plant phenotyping. *BMC bioinformatics*, 14(1), 238.

[19] Paulus, S., Schumann, H., Kuhlmann, H., and Léon, J. (2014a). High-precision laser scanning system for capturing 3D plant architecture and analysing growth of cereal plants. *Biosystems Engineering*, 121, pp. 1–11.

[20] Paulus, S., Eichert, T., Goldbach, H. E., and Kuhlmann, H. (2014b). Limits of Active Laser Triangulation as an Instrument for High Precision Plant Imaging. *Sensors*, 14(2), pp. 2489–2509.

[21] Rose, J., Paulus, S., and Kuhlmann, H. (2015). Accuracy Analysis of a Multi-View Stereo Approach for Phenotyping of Tomato Plants at the Organ Level. *Sensors*, 15(5), pp. 9651–9665.

[22] Tester, M., and Langridge, P. (2010). Breeding technologies to increase crop production in a changing world. *Science,* 327 (5967), pp. 818–822.

[23] Werner, S., Neumann, I., Thienel, K. C.,and Heunecke, O. (2013). A fractal-based approach for the determination of concrete surfaces using laser scanning techniques: a comparison of two different measuring systems. *Materials and structures, 46(1–2)*, pp. 245–254.